Dynamic Changes During the Immune Response in T Cell–Antigen-presenting Cell Clusters Isolated from Lymph Nodes

Mirja Hommel and Bruno Kyewski

Tumor Immunology Program, Division of Cellular Immunology, German Cancer Research Center (DKFZ), D-69120 Heidelberg, Germany

Abstract

Activation of antigen-specific T cells by mature dendritic cells in secondary lymphoid organs is a key control point of the adaptive immune response. Here we describe the ex vivo isolation of preformed multicellular clusters between T cells and antigen-presenting cells. Adoptively transferred, antigen-specific T cells segregated into individual clusters where their activation and proliferation was initiated in vivo. Transit of the T cell cohort through the cluster compartment required 32–36 h. The precise timing of the response to agonistic epitopes was remarkably invariant regardless of the T cell lineage, the major histocompatibility complex haplotype, and the antigen dose. Interestingly, initiation of cell division of T cells specific for a subdominant epitope and a weak agonist was delayed by 6 h. The results provide a basis for the analysis of short range, mutual cell–cell interactions within such confined microenvironments.

Key words: cell-cell interaction • microenvironment • T cell activation • compartmentalization • dendritic cells

Introduction

Antigen-specific activation of T cells is the key event in the successful induction of an adaptive immune response. The antigen dose, the duration of antigen presentation, and the cellular and molecular environment in which antigen is presented will influence the fate of antigen-specific T cells. They will either be driven into effector cells or after transient proliferation, become anergic or die. A prime determinant in the decision between immunity and tolerance is the maturation stage of dendritic cells (DCs)* encountered by naive T cells. Pathogen-derived signals induce tissue-resident DCs to mature and migrate to local LNs where they present antigen to naive recirculating T lymphocytes. This professional competence for antigen presentation correlates with high expression of MHC, costimulatory (such as CD80 and CD86), as well as adhesion (intercellular adhesion molecules 1 and 3) molecules (1). Initial adhesion of T cells to DCs is antigen independent, allowing scanning

of specific antigen–MHC complexes by TCR (2). In the case of antigen recognition, an intracellular signaling cascade ensues in the T cell, which in turn promotes further maturation of DCs and eventually results in clonal proliferation of T cells and their differentiation into effector cells (3).

While this sequence of events is undisputed, many cellular and molecular aspects of early T cell priming remain undefined or controversial. Thus, experimental data concerning the minimal duration of cell–cell contact differ widely. In vitro, brief interactions (<1 h) have been reported to initiate an autonomous differentiation program in CD8 T cells resulting in six to eight cell divisions (auto pilot model; reference 4). On the other hand, prolonged T cell–APC contact (up to 24 h) has been reported to be necessary to irreversibly commit T cells to differentiation into effector cells (5, 6). Parameters determining this time interval include the affinity of the T cell receptor for surface MHC–peptide complexes as well as the epitope density on DCs. It has been shown that T cells responding to high versus low affinity TCR ligands differ in the onset of proliferation (7) whereas T cells specific for dominant versus subdominant epitopes expand with the same kinetics, but differ in the extent of proliferation (8).

Another contentious issue is the mode of signaling: is continuous signaling during a single T cell–DC encounter required to irreversibly activate T cells or are short signal-

ing spells during sequential interactions sufficient? Performing long-term time-lapse video microscopic analyses in extracellular collagen matrices, Gunzer et al. (9) showed that T cell–DC contacts were short (2–3 min) and did not differ between unpulsed and antigen-pulsed DCs. Yet, these sequential, short-lived and dynamic, antigen-specific T cell–DC contacts rapidly induced cytoplasmic calcium influx and T lymphocytes were effectively activated as measured by blast formation and up-regulation of CD69 and CD25. How efficient is scanning of DCs by rare antigen-specific T cells considering that only a fraction of DCs in T cell areas might be loaded with the respective antigen (10, 11)? Does stable and prolonged immunological synapse formation occur in vivo at the interface between DCs and T cells only upon recognition of agonist T cell epitopes?

Static interactions of T cells with DCs in vivo and in vitro had been known for a long time (12, 13). Since then, these cell–cell interactions have been analyzed in great detail in vitro and more recently in situ. Thus, injection of superantigens (14) or allogenic cells (15, 16) resulted in localization of activated T cells adjacent to DCs. A more detailed in situ analysis of clonal or polyclonal T cell populations during the immune response has only recently become amenable to experimental analysis. Using a T cell receptor transgenic (tg) model, clusters of proliferating T lymphocytes have been shown to localize closely to DCs that were either antigen loaded and adoptively transferred or virally infected in vivo (17, 18). Recently, elegant studies extended this approach to the in situ analysis of the dynamics of T–DC interactions in various models applying novel imaging techniques (19, 20).

While these pioneering in vivo studies insinuate specific interactions between T and DCs, they do not allow the delineation of those T cells that physically interact with DCs from those that merely colocalize with DCs. To monitor stable physical T cell–DC interaction in vivo, we resorted to the ex vivo isolation of preexisting T cell–APC clusters. This approach has been previously applied to delineate sequential cell–cell interactions during intrathymic development (21). Our results characterize such multicellular T cell–APC clusters as the LN microenvironment of T cell priming and provide a basis for additional detailed analysis of these multicellular units.

Materials and Methods

Mice. Mice of the inbred strains C57BL/6 (H-2^b) and BALB/c (H-2^d) were obtained from Charles River Laboratories and kept under specific pathogen-free conditions. Dep- and Sep-TCR tg mice in which CD4$^+$ T cells express a TCR recognizing either a dominant (Dep) or a subdominant (Sep) epitope of the human C–reactive protein (hCRP) in the context of H-2^b have been previously described (22). They were bred in our animal facilities. OT-I and OT-II TCR tg mice specific for chicken OVA in the context of H-2^b (23, 24) had been bred on the C57BL/6 background for more than 10 generations and were provided by A. Limmer (University of Heidelberg, Heidelberg, Germany). DO11.10 mice, which recognize the dominant OVA peptide

323–339 in the context of H-2^d (25), were provided by A. Schimpl (University of Würzburg, Würzburg, Germany).

Antibodies. The following monoclonal antibodies were used in this study: R613–anti-CD4 (H129.9) and R613–anti-CD8 (53-6.7; both from GIBCO BRL); FITC–anti-Vβ5.1,5.2 (MR 9-4), FITC–anti-Vβ8.3 (1B3.3), PE–anti-CD62L (Mel-14), PE–anti-CD69 (H1.2F3), CyChrome–anti-CD4 (H129.19), and biotin–anti-CD11c (HL3; all from BD Biosciences/Becton Dickinson); and biotin-anti–follicular DC (FDC; FDC-M2; AMS Biotechnology). Biotinylated antibodies were detected with Alexa 488– (Molecular Probes), Cy3-, or Cy5-conjugated streptavidin (Dianova).

Antigens. hCRP was provided by M.B. Pepys (Royal Hospital, London, United Kingdom) or obtained from Sigma-Aldrich. Chicken OVA grade 5–6 was also obtained from Sigma-Aldrich. Peptides were synthesized in the core facilities at the DKFZ. For stimulation of OVA-specific T cells, either complete OVA, OVA-peptide$_{257–264}$ (SIINFEKL), or the weak agonist SIINFEDL (variant D7) were used (26). The peptides were dissolved in DMSO at a concentration of 10 mg ml^{-1} (stock solution).

Flow Cytometry. Expression of cell surface antigens was detected by flow cytometric analysis. For staining, enriched cell clusters were dissociated by incubation with 25 mM EDTA for 5 min at 37°C before staining. For analysis, data of 10,000 stained cells were measured with a FACScan™ (Becton Dickinson) and analyzed with CELLQuest™ (Becton Dickinson) or FlowJo® research software (Tristar, Inc.). Nonlymphoid and dead cells were excluded by appropriate forward- and side-scatter gating.

Cell Tracking. Cells to be intracellularly stained with 5(and 6)-carboxyfluorescein diacetate succinimidyl ester (CFSE) were washed twice with PBS and then resuspended at 1–5 × 10^7 cells ml^{-1}. CFSE (Molecular Probes) was added to a final concentration of 2 μM and the suspension was incubated at 37°C for 10 min. Cells were then washed twice. To assess T cell proliferation, clusters were dissociated and analyzed. 50,000–100,000 events were collected for data analysis.

Cells to be stained with 5-(and-6)-(((4-chloromethyl)benzoyl)amino)tetramethylrhodamine (CMTMR; CellTracker™ Orange; Molecular Probes) were washed twice in PBS and then resuspended at 1–5 × 10^7 cells ml^{-1}. CMTMR was added to a final concentration of 1 μM and the suspension was incubated at 37°C for 30 min. The reaction was stopped by adding cold PBS. After washing, the cells were incubated for another 30 min to allow all dye to be converted. Cells were then washed twice. Dead cells and debris cells were removed by filtration through a 30-μm nylon mesh (Nybolt).

Immunizations. Mice were anesthetized by inhalation of Metofane (Janssen-Cilay) and immunized into the hind footpads with a 1:1 mixture of antigen/PBS and CFA, total volume 50 μl/foot. Each mouse received 50–100 μg antigen.

T Cell Transfers. Spleen and mesenteric LN cells of TCR tg mice were prepared as single cell suspensions and pooled. After erythrocyte depletion, cells were analyzed for the frequency of TCR tg T lymphocytes by flow cytometry. The number of transferred cells was adjusted to 4–5 × 10^6 tg cells/mouse, resuspended in 200 μl PBS, and adoptively transferred intravenously into C57BL/6 or BALB/c mice. Likewise, transfers were performed with intracellularly stained cells. The frequency of tg T cells before transfer ranged between 10 and 30% of total splenocytes.

T Cell Enrichment by MACS. CD4$^+$ and CD8$^+$ T cells were enriched by depleting complementary lymphoid subsets using MACS according to the manufacturer's protocol (Miltenyi Biotec). In short, 10^8–10^9 cells were incubated with a cocktail of

anti–CD8–biotin or anti–CD4–biotin, respectively, (both from GIBCO BRL), anti–F4/80–biotin (ourselves), and anti–CD11c–biotin (BD Biosciences/Becton Dickinson) antibodies for 15–20 min on ice. After washing, anti–B220 and streptavidin microbeads (Miltenyi Biotec) were added for another 15–20 min on ice. Separation was performed as described with a MidiMACS (Miltenyi Biotec). Enrichment was verified by flow cytometry.

Preparation of T Cell–APC Clusters. Preparation of LN clusters was performed with modifications as previously described (21). In short, LNs were removed, freed of connective and fat tissue, the capsule was cut open, and the tissue was gently stirred for 3–5 min at 27°C to release the bulk of free cells. Tissue fragments were allowed to settle, free cells were removed, and the fragments were digested three to five times (10 min at 27–37°C) with 0.2 mg ml^{-1} collagenase/dispase buffer grade I (Boehringer/Roche Diagnostic), 0.2 mg ml^{-1} collagenase grade IV (Interchem), 50 μg ml^{-1} DNase I (ICN Biomedicals), 12 trypsin inhibitor units (TIU)/mg aprotinin, RPMI 1640 supplemented with 2% FCS and 20 mM Hepes. Clusters were enriched by sedimentation at unit gravity through FCS (two times for 10–45 min at 4°C) attaining a purity of 1:1 to 1:10 clusters per free cell.

Immunofluorescence Microscopy. After surface staining and fixation with 2% paraformaldehyde, T cell–APC clusters were analyzed microscopically. One- or two-color analysis was performed with a Zeiss Axiophot II (Wetzlar) whereas three-color staining was analyzed with a confocal microscope (Zeiss LSM510; Carl Zeiss MicroImaging, Inc.). Data were documented with AXIO-VISION 3.0 software (Carl Zeiss MicroImaging, Inc.).

Online Supplemental Material. Fig. S1 shows different CD62L expression levels on free and cluster-associated T cells defining regions on which the definition of high and low expression was based. Fig. S2 shows a replicate experiment of the type depicted in Fig. 4 a. Fig. S3 shows the frequency of Sep T cells in CFA-reactive local LNs in the absence of specific antigen. The online supplemental figures are available at http://www.jem.org/cgi/content/full/jem.20021512/DC1.

Results

Isolation Ex Vivo and Characterization of Lymphocyte–Stromal Cell Clusters. The method of preparing T cell–APC clusters from thymus has been previously described (21). Here, this method has been adopted to obtain such clusters from LNs in high purity. The average number of lymphocytes clustered around each APC was 10–20 as determined by dissociation of highly purified clusters and subsequent enumeration of stromal cells and lymphocytes. Four types of clusters could be isolated from regional LNs that differed clearly with respect to their lymphoid and stromal cell composition. CD11c$^+$ DCs formed clusters with T cells only (∼10% of all clusters), B cells only (∼15%), and mixed T/B clusters (∼20%; Fig. 1, a, b, and d). In addition, B cells formed clusters with M2$^+$ FDC (∼55%; Fig. 1 c). The ratio of B cell clusters formed by FDC versus DCs was 4 to 1. Thus, although T cells were found to associate only with DCs, only a minority of B cells interacts with DCs. The latter interactions most likely represent the associations between plasmablasts and myeloid DCs in the
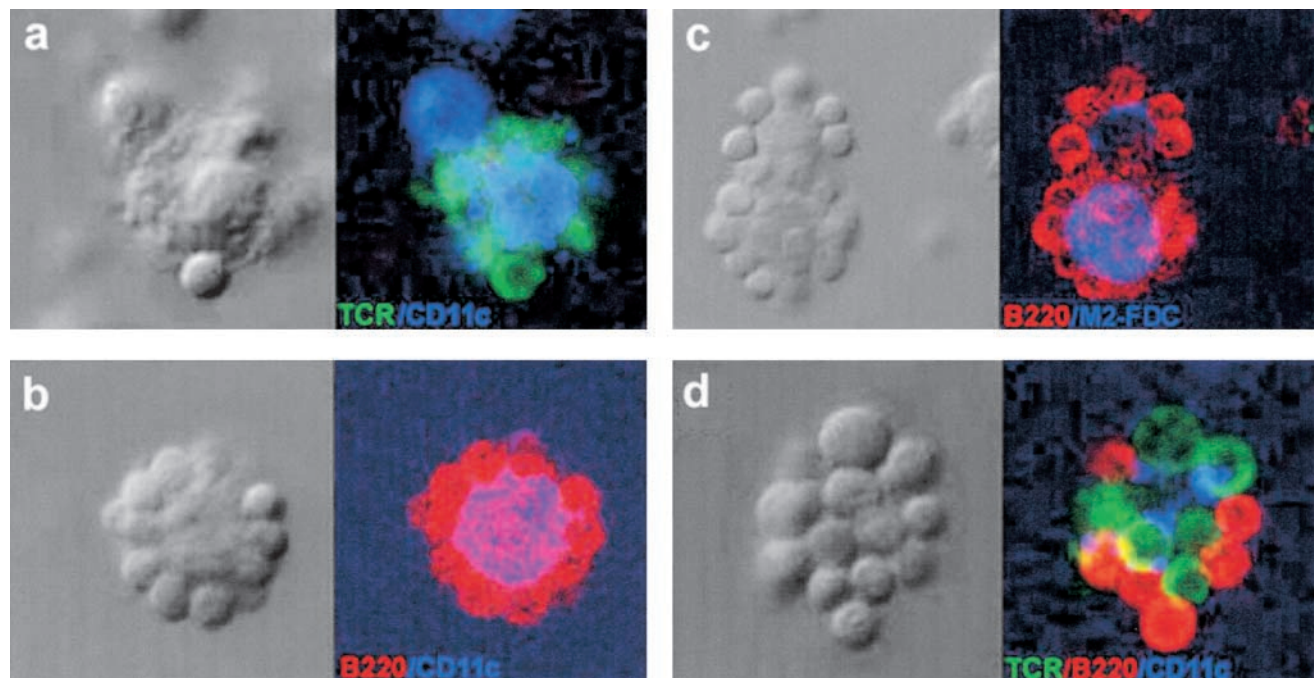

Figure 1. Cluster composition. Clusters were prepared from the draining LNs of CFA-immunized animals 4–5 d after immunization. (a) T cells form clusters with CD11c$^+$ DCs. (b and c) B cells form tight clusters both with CD11c$^+$ DCs (b) and M2$^+$ FDC (c). (d) mixed B and T cell cluster with CD11c$^+$ DCs. Note that some B cells appear to attach to T cells rather than DCs. Purified clusters were stained with (a) anti–CD3ε–FITC/anti–βTCR–FITC and anti–CD11c–biotin/sav–Cy-5, (b) B220–PE and anti–CD11c–biotin/sav–Cy5, (c) B220–PE and anti–FDC–biotin/sav–Cy-5, and (d) anti–CD3ε–FITC/anti–βTCR–FITC, anti-B220–PE, and anti–CD11c–biotin/sav–Cy-5. A detailed composition of cluster-associated lymphocytes is provided in Table S1, available at http://www.jem.org/cgi/content/full/jem.20021512/DC1.

271   Hommel and Kyewski

junction zone between T and B cell areas as previously described (27, 28). The majority of LN clusters after immunization were formed by B cells probably owing to a strong B cell response induced by CFA. (A detailed composition of cluster-associated lymphocytes is provided in Table S 1, available at http://www.jem.org/cgi/content/full/jem.20021512/DC1; reference 29).

Cluster formation in vivo was not strictly dependent on deliberate antigen administration. It was also possible to isolate them in lower numbers from LNs of unprimed mice, in which "natural," noninduced immune responses are likely to occur. The yield of clusters obtained from immunized animals, which additionally received antigen-specific T cells, was higher than that from mice only immunized with CFA with or without additional antigen. The yield of clusters ranged between 7×10^3 per mesenteric LN in nonimmunized mice to 32.6×10^3 per pooled inguinal and popliteal LN after immunization and T cell transfer (Table I). At least 10% of all T and B cells are engaged in these cell–cell interactions at a given time point based on the total number of lymphocytes, the frequency of cluster, and an average number of 15 lymphocytes per cluster. This represents a minimal estimate due to certain loss of clusters during the enrichment procedure and disintegration during in vitro handling. Thus, clusters form in the absence of deliberate immunization, however, their formation is clearly enhanced by an ongoing local immune response.

Antigen-specific T Cells Segregate into Clusters. To further document the role of these clusters in the antigen-specific T cell response we analyzed whether or not antigen-specific T cells preferentially segregate into such clusters and whether they partition into individual APCs or distribute equally within clusters. To this end, we transferred CFSE prelabeled antigen-specific T cells into primed mice and followed their fate by microscopic analysis.

We used a TCR tg mouse model, in which the tg TCR recognizes either a Dep or Sep epitope in the context of I-A^b (22). C57BL/6 mice were immunized with antigen in CFA and 4 d later received CFSE-labeled Sep tg T cells intravenously. At the indicated time points after transfer, 100

CD11c$^+$ clusters were assessed for the number of labeled T cells they contained. Fig. 2 depicts one representative out of three experiments. Although at all time points analyzed a large proportion of clusters did not contain any CFSE-labeled cells, the proportion of clusters with two or more associated CFSE$^+$ T cells increased over time. 36 h after transfer, the proportion of clusters containing three or more CFSE$^+$ cells was maximal and decreased thereafter. The coexistence of clusters devoid of any transferred cells and clusters with more than three donor cells accounts for a segregation of T cells into clusters. Considering an average number of 10–20 T cells per cluster, 3 or more CFSE-stained T cells/cluster equal $\geq 15\%$. In comparison, only 5% of cells in the nonclustered fraction were CFSE$^+$ at this time point. Hence, there was a more than threefold enrichment of antigen-specific lymphocytes into individual T cell–APC clusters. This segregation was not seen after immunization with the control antigen ovalbumin (Fig. 2 b) and thus is the result of specific antigen recognition.

Cluster-associated T Lymphocytes Display a Distinct Phenotype. Does this preferential segregation of antigen-specific T cells into clusters correlate with a distinct T cell phenotype either as a prerequisite or a consequence of these interactions? We first assessed expression of the homing receptor CD62L, which is highly expressed on naive recirculating T cells. CD62L is transiently down-regulated upon LN entry through high endothelial venules. There-

Table I. *Recovery of Lymphocyte–APC Clusters*

	Cluster number ($\times 10^{-4}$)	Cluster/mg LN tissue[a]
mes LN	0.72 ± 0.2	463
CFA only	1.48 ± 0.4	543
CFA + Ag	1.40 ± 0.3	538
CFA + Ag + T cell transfer	3.26 ± 2.3	913

Cluster numbers represent the mean ±SD of at least three to five mice. Clusters from nonimmunized animals were prepared from mesenteric LNs (mes LN). The low yield of clusters from local LNs precluded a precise enumeration. Clusters from immunized mice were prepared from pooled inguinal and popliteal LNs.
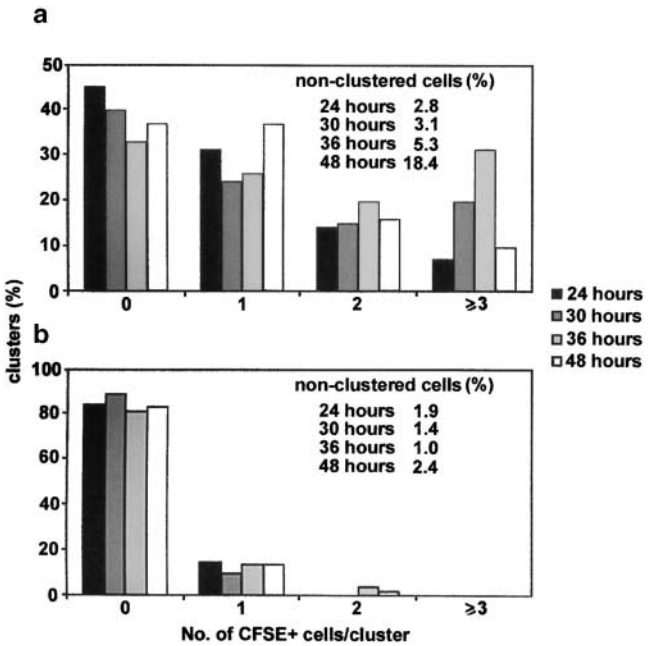[a]Calculated from mean values.

Figure 2. Antigen-specific T cells segregate into individual clusters. Mice were immunized with 50 μg hCRP/CFA (a) or 50 μg OVA/CFA (b) and then received 5×10^6 CFSE-labeled Sep-specific T cells. Clusters were prepared from regional LNs at the indicated times and analyzed by fluorescence microscopy. 100 clusters were scanned randomly and the number of CFSE-stained T cells/cluster was determined. For comparison, the frequencies of nonclustered cells are shown. For each time point LNs of two mice were pooled. One representative out of three experiments is shown for a and one control experiment was performed for b.

fore, low CD62L expression may denote recent arrivals among T cells (30). Clusters were isolated from the draining LNs of immunized animals, which had been subsequently transferred with unstained, antigen-specific lymphocytes. These lymphocytes were then identified by expression of the respective tg TCR Vβ chain and the appropriate coreceptor. Intriguingly, cluster-associated lymphocytes displayed a much lower level of CD62L expression than their free counterparts (Fig. 3 a and Fig. S1, available at http://www.jem.org/cgi/content/full/jem.20021512/DC1). This finding was confirmed in four different transfer models (see below) including CD4 and CD8 T lineage cells as well as in animals immunized with CFA only (unpublished data).

The activation status of clustered T cells was evaluated by measuring CD69 expression levels. This early T cell activation marker is up-regulated within 2–6 h after TCR triggering (31). Up-regulation of CD69 on cluster-associated T cells would indicate that the interaction time is longer than the time required for up-regulation of CD69. Interestingly, strong CD69 up-regulation could be observed on cluster-derived tg T cells but not (or to a far lesser degree) on clustered, non-tg, or free T cells (Fig. 3 b), clearly indicating activation of antigen-specific T cells within clusters.

T Cell Proliferation Is Initiated in T Cell–DC Clusters. Next, we analyzed whether activated T cells proceeded to the first T cell division while still in contact with the APC. To dissect the proliferation kinetics of Dep and Sep, T cell–APC clusters were prepared at different time points and assessed for T cell proliferation by CFSE dilution analysis. 24 h after transfer, both populations could be detected in the draining LNs as well as in clusters as single cells, but T cell division could not yet be observed (Fig. 4). Forward/side scatter analysis revealed that most transferred

cells were small with incipient blastogenesis detectable in the cluster fraction, but not among nonassociated ("free") lymphocytes. For Dep-specific T cells, the first division, measured as CFSE fluorescence halving, could be observed at 30 h in the cluster fraction, but at this time point not yet in the fraction of free lymphocytes. Within the next 24 h an increase in blasts occurred in both fractions and was accompanied by continuing cell division. Furthermore, 36 h after transfer the relative proportion of CFSE-stained cells in the total population as well as in the blast fraction of dissociated lymphocytes was higher than in the free ones (30.7 ± 9.9% vs. 20.4 ± 1.1%; P < 0.05), thus reflecting an enrichment of antigen-specific blasts within clusters. At 48 h a cohort of cells had divided four times, corresponding to an average division time of 4.5 h. At the same time, fractions of cells had divided less than four times and these cohorts were of similar size (Fig. 4, left panels, and Fig. S2, available at http://www.jem.org/cgi/content/full/jem.20021512/DC1). At this time point, the preponderance of blasts in clusters could not be found anymore and now the relative proportion of CFSE-stained cells within the blast fraction was about twice as high in free cells as in the dissociated ones (41.4 ± 9.2% vs. 24.9 ± 6.9%; P < 0.01). 72 h after transfer, the proportion of CFSE-stained cells within the blast population started to decrease in the cluster fraction but continued to increase in the fraction of free lymphocytes (unpublished data). These results document an initial onset of proliferation while the T cells are still in contact with the APC, followed by a "cluster-independent" cell division phase.

Interestingly, even though T cells specific for a subdominant epitope of hCRP could also be localized in clusters at 24 h, the first division of these cells lagged ∼6 h behind that of cells specific for the dominant epitope (Fig. 4). It should be pointed out that despite a later appearance of the
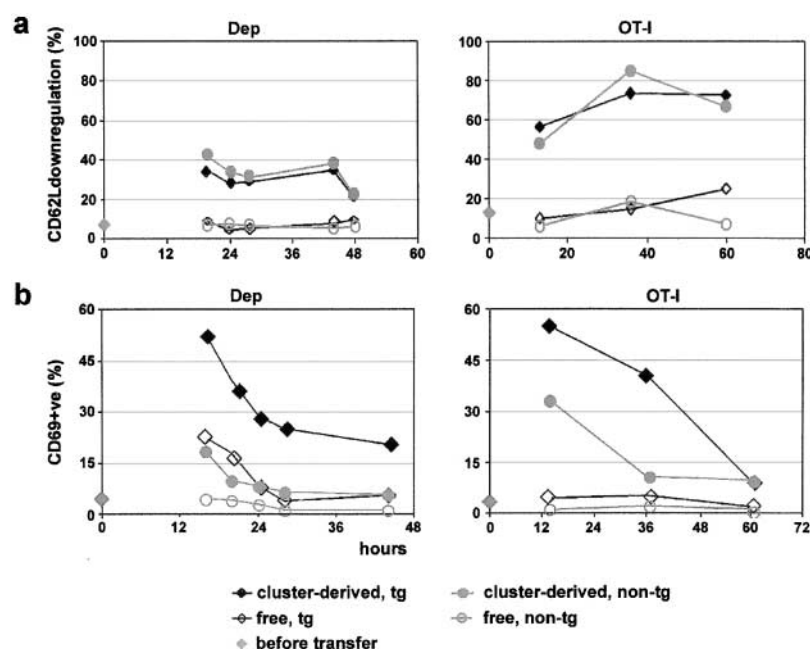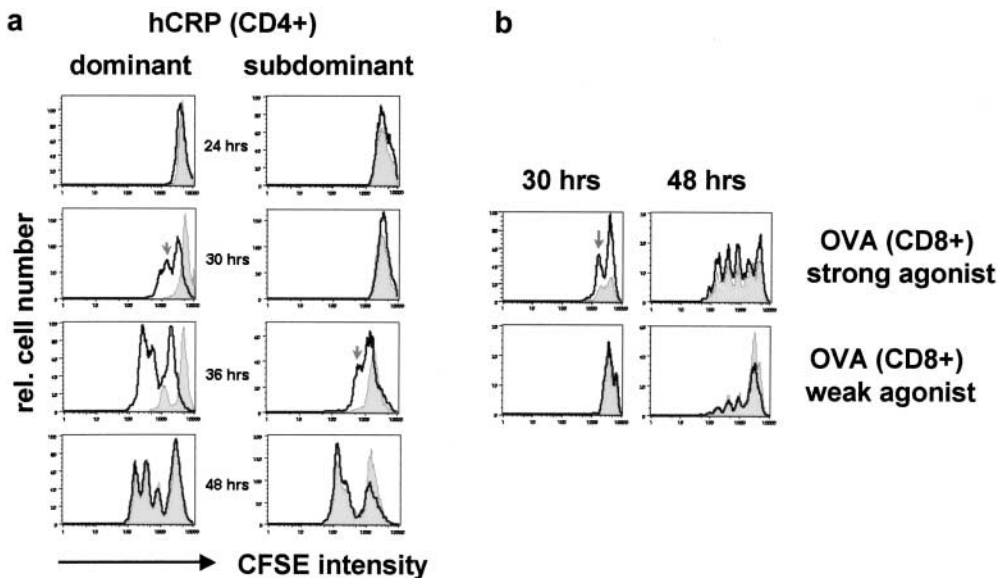

Figure 3. A distinct phenotype of clustered T lymphocytes. Mice were immunized with 50 μg antigen/CFA and 4 d later received 5 × 10⁶ tg, unlabeled T cells intravenously. Clusters were prepared from the regional LNs at the indicated time points after transfer. Cluster-associated and nonassociated cells were then analyzed for CD62L (for expression levels of CD62L, see Fig. S1, available at http://www.jem.org/cgi/content/full/jem.20021512/DC1) (a) and CD69 expression (b). Transferred cells were identified by expression of their tg TCR Vβ chain and the corresponding coreceptor. In clusters, T cells displayed lower levels of CD62L expression regardless of antigen specificity whereas tg CD4⁺ cells preferentially showed up-regulation of CD69. 20,000 events were analyzed.

Figure 4. T cell proliferation is initiated in clusters. (a) Mice were immunized with 50 μg hCRP/CFA and then received 5 × 10⁶ CFSE-labeled Sep- or Dep-specific T cells intravenously. Cluster-derived and nonassociated cells were analyzed for CFSE dilution at the indicated time points. Note that T cell proliferation was initiated in the cluster-associated fraction and that there was an epitope-dependent shift in the timing of the first T cell division. Representative of three to four independent experiments (see also Fig. S2, available at http://www.jem.org/cgi/content/full/jem.20021512/DC1). (b) Mice were immunized with 50 μg SIINFEKL/CFA (strong agonist) or SIINFEDL/CFA (weak agonist) and then received 5 × 10⁶ CFSE-labeled OVA-specific OT-1 T cells intravenously. The strong and weak agonists differed with respect to the kinetics and extent of proliferation. Black lines depict the cluster-associated fraction, gray filled histograms depict the respective nonassociated cells. The analysis included "blasts" and small lymphocytes. 100,000 events were collected. The arrow marks the first detectable cell division. CFSE⁻ cells are not shown.

first T cell division, some Sep-specific T cells had also divided four times 48 h after transfer. Apart from the 6-h lag in the onset of proliferation, the same proliferation pattern was observed for both epitopes. Notably, proliferation of Sep tg cells was less vigorous, i.e., the average relative proportion of CFSE-labeled T cells found in the blast fraction was higher for Dep tg cells than for Sep tg ones (at 48 h, Dep: 41.4 ± 9.1% [free] vs. 24.9 ± 6.9% [cluster-derived]; Sep: 17.0 ± 3.2% [free] vs. 14.0 ± 1.4% [cluster-derived]).

Clonal Expansion Requires a Threshold Dose of Antigen. The delayed onset of proliferation of T cells specific for the subdominant epitope might be attributed to different densities of epitope display or distinct TCR affinities of the TCRs for their respective epitopes. Presentation of the naturally processed dominant epitope has been shown to

be 100-fold more efficient than that of the subdominant epitope (32, 33). If lower peptide density was responsible for the delayed kinetics, a reduction in antigen dose should mimic such a situation. Hence, the kinetic analysis was performed in mice that had received decreasing amounts of hCRP.

Lowering the dose of hCRP from 25 μg/mouse to 0.5 μg/mouse did not affect the time point of completion of the first T cell division of either population. However, at an antigen dose of 0.1 μg/mouse or below, proliferation could no longer be detected (Fig. 5). At such low doses, antigen-specific cells seem to transiently accumulate in clusters but do not receive stimulation strong enough to trigger T cell activation ("abortive stimulation"). Likewise, the extent of proliferation was not affected by the dose
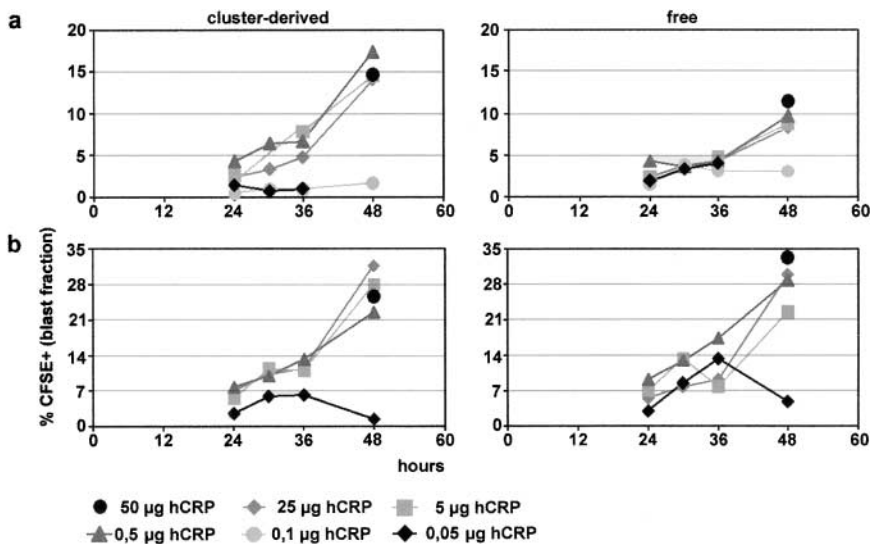

Figure 5. A threshold dose of antigen is critical for T cell proliferation. BL/6 mice were immunized with varying doses of hCRP/CFA and then received 5 × 10⁶ CFSE-labeled Dep- (a) or Sep-specific T cells intravenously (b). Cluster-derived and nonassociated cells were analyzed for the frequency of CFSE-labeled cells among the blast fraction. The T cell response required a minimal dose of 0.1–0.5 μg antigen/mouse. Above this dose the kinetics and the extent of proliferation were insensitive to additional augmentation. The response to 50 μg is shown for the 48-h time point.

274   T Cell–APC Interactions in Lymph Nodes

variation, i.e., proliferation of Sep tg lymphocytes was always lower than that of Dep tg ones. Thus, both T cell populations are highly sensitive to low antigen dose. Below a certain threshold no proliferation takes place whereas above this threshold, antigen augmentation did not affect the outcome of the response as analyzed here.

T Cell Response Kinetics Do Not Vary with the Model Antigen. Having defined the kinetics of the early T cell response in the hCRP model to high resolution, we asked to what extent the particular TCR and its specific peptide/MHC ligand influence the response. Hence, we conducted the same analysis in two other TCR tg models of the CD4 lineage, the OVA/OT-II model, also restricted by H2[b] (23), as well as the OVA/DO11.10 model restricted by H-2[d] (25). Like hCRP-specific T cells, OVA-specific T lymphocytes could be detected within clusters 24 h after transfer in these two models. Moreover, completion of the first T cell division was observed at 30 h for both OT-II and DO11.10 tg T cells, comparable to the Dep-specific population. Again, the proliferation kinetics in the cluster-associated fraction preceded that in the nonassociated cell fraction. At 48 h, cells of both fractions had undergone the same number of divisions (unpublished data). Thus, regardless of the TCR/ligand pairing, the dynamics of CD4 T cell–APC interactions in situ were comparable.

Because various reports emphasized differences between CD4 and CD8 T cells in their activation requirements and their degree of clonal expansion (4, 34), we also included a CD8 response in our study using the OT-I tg mice. In this well characterized model, the tg TCR recognizes the dominant OVA peptide$_{257-264}$ (SIINFEKL) in the context of H-2[b] (22). Similar to the hCRP/Dep model, these T cells had readily localized in clusters by 24 h after transfer. At 30 h, the first T cell division had taken place (Fig. 4). Proliferation continued during the following 18 h, but in contrast to the CD4 models, the percentage of CFSE-labeled cells in the cluster-derived fractions remained above that of the nonassociated fraction. Thus, CD4+ and CD8+ T cells behaved similarly with regard to the kinetics of T cell–APC interactions, but, at least in case of the OT-I model, the transition time of CD8+ T cells through the cluster compartment is apparently longer.

The onset of T cell proliferation in response to immunization turned out to be a remarkable constant parameter regardless of the T cell lineage or the MHC haplotype, when lymphocytes responding to a dominant (strong ago-

nist) epitope were analyzed. 30 h after cell transfer, the first round of cell division was initiated in a fraction of cells, only in the case of a subdominant epitope, a delay of ∼6 h was observed. The OVA/OT-I model offers the particular advantage that a series of peptide derivatives has been defined with properties ranging from strong agonists to antagonists. These variants allow the effect of TCR signal strength on the T cell response in situ to be analyzed. We chose the OVA peptide$_{257-264}$ variant D7 (SIINFEDL), which carries an aspartic acid instead of a lysine at position 7 to address this question (26). After transfer into SIINFEDL-immunized mice, OT-1 tg T cells could again be detected in clusters 24 h after transfer. Proliferation of the majority of antigen-specific T cells was not apparent before 36 h in contrast to clusters prepared from control animals that had been immunized with the strong agonist SIINFEKL. In addition, the relative and absolute numbers of cells taking part in the response to the weak agonist were lower than to the strong agonist (Fig. 4). Thus, the weak agonist shows a delayed kinetics and a reduced number of cells proliferating in the antigen response.

Average Transit Time through the Cluster Compartment. Compilation of the kinetic analyses in the different models allows an estimate of the mean transit time of transferred T cells through the "cluster compartment" in the course of an antigen response. As shown for the hCRP model, T cells could first be detected 12–16 h after transfer in clusters. After 30–36 h a fraction of T cells had completed their first round of cell division. After rapid expansion they reached their maximal increase within clusters 48 h after transfer and declined thereafter. The transit time through this cluster compartment is thus ∼36 h. The same kinetics are mimicked by nonassociated T cells with a phase shift of 6–12 h indicating that expansion, after being initiated within cluster, then becomes cluster independent (Fig. 6 and Fig. S3, available at http://www.jem.org/cgi/content/full/jem.20021512/DC1). This pattern has been observed in all CD4 models with OT-I CD8 T cells showing a more protracted exit from the cluster compartment. While these considerations apply to transferred T cells as a whole population, we cannot track the fate of individual cells by this analysis.

Lymphocyte Subsets Colocalize in Individual Clusters. Lymphocyte–APC clusters containing at least three different T cell types have been postulated as the minimal unit underlying cognate T–T and T–B cell interactions, which could
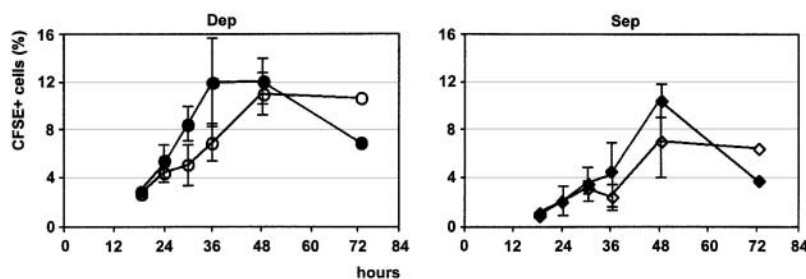

Figure 6. T cell transit through the cluster compartment. Compiled data of the kinetics of the antigen response of Dep and Sep T cells. ○ and ◇ represent the nonassociated fractions and ● and ◆ represent the cluster-derived fractions. Note the phase shift in the response between both compartments. The fraction of CFSE+ lymphocytes of at least three independent experiments (only one experiment for the 72-h value) with two to three mice per time point is shown. There was no expansion in the absence of antigen (Fig. S3, available at http://www.jem.org/cgi/content/full/jem.20021512/DC1).

result either in help, suppression, or immune deviation (35, 36). To formally demonstrate the existence of such clusters in vivo, we cotransferred CD4 T cells (Sep and Dep) specific for two epitopes of the same protein antigen (hCRP), CD4 and CD8 T cells (Dep and OT-I) specific for two different antigens (hCRP and OVA, respectively), and CD8 and CD4 T cells (OT-I and OT-II, respectively) specific for the same antigen (OVA). The two T cell subsets were tracked with red and green intracellular dyes after transfer in equal numbers into mice preimmunized with the relevant antigen. Clusters were isolated 30 h after transfer and stained with anti-CD11c or anti–MHC class II mAb. In each case the different combinations of T cells were found to colocalize in individual DC clusters (Fig. 7). Clusters

harboring both subsets were less frequent than those with one subset only. In the case of two populations recognizing the same protein antigen, the proportion of clusters containing both subsets was higher (∼1 in 20) whereas T cells of different protein specificities colocalized less frequently.

Given the colocalization of T cells of different specificities within the same APC cluster, we asked whether the response of one population would be influenced when a second population recognizing a different epitope of the same antigen was cotransferred. When 5×10^6 CFSE-labeled Sep T cells were transferred with or without the same number of unlabeled Dep T cells, no difference in the onset and extent the Sep response was apparent. The same was true for the reverse combination under these experimental conditions (unpublished data).

Discussion

Successful induction of an adaptive immune response is determined by the context in which antigen is presented, its dose, and the duration of its presentation (37). These parameters are governed by the microenvironment of secondary lymphoid organs in which T cell priming occurs, its cellular composition, and dynamic changes during the antigen response. Here we present evidence that such in situ microenvironments can be isolated intact from LNs as multi-cellular clusters and further analyzed in vitro. This approach reduces the complexity of the unperturbed organ to less complex subdomains of the microenvironment, which are amenable to further analysis and manipulation at the single cell level in vitro. This way, differentiation steps, which are governed by the topology of interaction partners via direct cell–cell interactions or short-range soluble factors, can be analyzed with high precision. Compared with the in situ analysis, extraction of clusters from pooled LNs provides a larger sample size of interacting T or B cells and thus a higher degree of sensitivity is achieved. Thus, both approaches should yield complementing information when judiciously combined.

In this study, we focused on the early priming phase of antigen-specific T cells. We observed a twofold increase in the numbers of clusters per tissue weight when immunized mice received antigen-specific T cells, thereby documenting a positive correlation between the relative density of clusters and an ongoing antigen-specific immune response. Transferred T cells were found to preferentially partition into the pool of clustered cells compared with free cells during the early phase of the response. Moreover, within the cluster pool, there was a clear segregation into individual clusters. T cell activation (i.e., up-regulation of CD69) and cell division were first detectable in the cluster fraction. These findings concur well with the in situ analysis of the interactions of host T cells with donor DCs in hepatic LNs of the rat (16). While the activation of T cells within clusters was essentially confined to antigen-specific tg T cells, reduced CD62L expression was a characteristic of most cells associated with clusters regardless of antigen specificity or cell transfer. The homing receptor CD62L has been
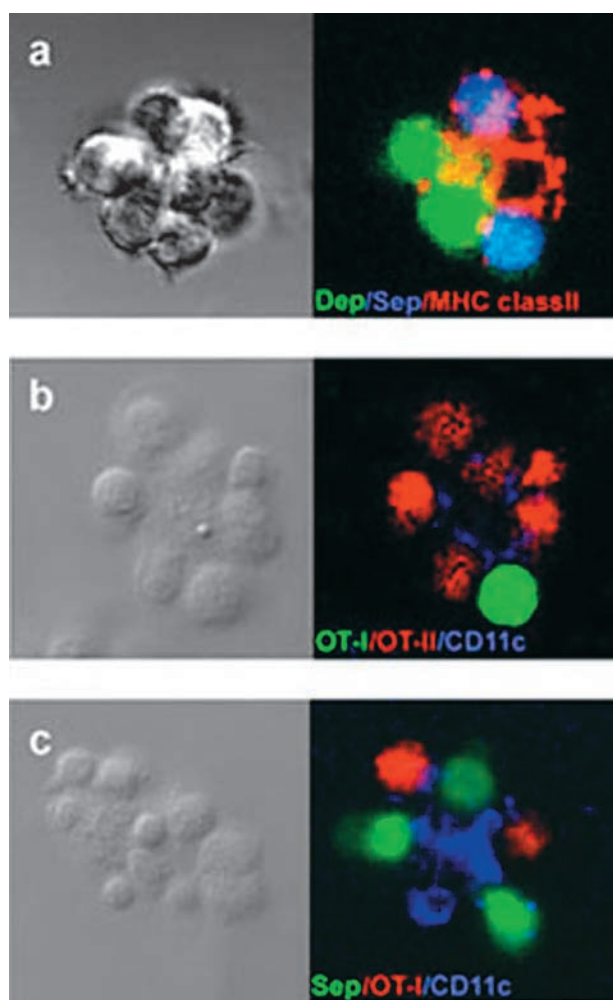

Figure 7. Different T cell subsets colocalize in individual clusters. Different pre-enriched and prelabeled tg T cell populations were adoptively transferred into animals previously immunized with the respective antigens. Clusters were isolated 30–36 h after transfer. (a) hCRP-specific Sep (blue) and Dep (green) T cells colocalize to the same MHC class II+ (red) stromal cell, (b) OVA-specific CD8 OT-I (green) and CD4 OT-II (red) colocalize to the same DC (blue), and (c) T cells with different protein antigen specificities, Sep (red) and OT-I (green), colocalize to the same DC (blue).

shown to be transiently down-regulated after transit through high endothelial venules and after T cell activation (30, 38). Lower levels of CD62L may thus denote recent LN immigrants or recently activated T cells. The discordant regulation of CD62L and CD69 expression favors the former interpretation and entry into T cell areas might be promptly followed by the scanning of DCs. The selective composition of these clusters supports the contention that they preexist in vivo and are not secondarily formed during isolation as previous studies on analogous clusters of the thymus already documented (21).

In a previous study by Ingulli et al. (17), fluorescent-labeled, antigen-loaded DCs and naive TCR tg CD4$^+$ cells specific for an OVA/H2^d complex had been adoptively transferred in vivo by confocal microscopy. In LN sections, OVA-specific T cells were shown to form clusters around paracortical DCs. These aggregates of antigen-specific T cells comprising ∼10–20 cells were of similar size as those we observed. Similarly, the peak of T cell clusters in situ and ex vivo was observed 48 h after transfer followed by dispersal of the T cells.

The timing of T cell activation and proliferation determined here in different tg models matches the findings of two recent studies using confocal laser video microscopy to follow the fate of antigen-specific T cells during priming in situ (19, 20). In the study by Stoll et al. (19) using the 5C.C7/B10.A TCR tg model specific for pigeon cytochrome C, T cells were found to localize to antigen-loaded DCs as small single cells and remained in contact for at least 15 h, the maximal observation period. T cell activation (CD69 up-regulation) occurred when T cells were still in contact with DCs and the first cell divisions were recorded 37 h after transfer. Moreover, the different in situ analyses (11, 16–20) and a previous in vitro analysis (5) accord well with a time window of ∼24 h between the lodging of T cells in the local LNs and ensuing first division. A more contentious issue is whether T cells during this period require sustained cell contact or oscillate between engagement and disengagement as observed in vitro in collagen matrices (9) or suspension culture (39). The study by Stoll et al. (19) supports the former interaction mode at least in the outer cortex. The sequence of events observed within clusters in this study (i.e., small single cells followed by blasts and doublets) and the stability of the preformed cell–cell interactions during isolation also do not concur with short-term interactions in the range of minutes (9).

The timing of the first cell division within clusters was highly reproducible and invariant among different models. Antigen was applied 4 d before T cell transfer and thus antigen-laden, mature DCs were already available when T cells reached the local LNs. This may also explain why CD8 T cells, requiring a "licensed" DC, behaved very similarly to CD4 T cells. The variables determining the commitment to T cell proliferation include the time required to home to local LNs, reach antigen-presenting DCs, and engage a TCR-mediated signal of sufficient strength and duration. Given the high reproducibility and resolution of the kinetic analysis, the delay of ∼6 h in the onset of division

in response to a subdominant CD4 T cell epitope and a weak CD8 T cell agonist is significant. A possible explanation for this finding has been offered by a recent study (7). The OT-I T cell response toward a low versus high affinity TCR ligand was compared to early and late biochemical signaling events. Both the high affinity ligand OVAp and the low affinity variant ligand G4 were able to induce maximal CD69 up-regulation in vitro, but 1,000–10,000-fold higher doses of G4 were required to reach equivalent responses. The expression of CD69 was similar at 24 h but up-regulation in response to G4 was found to lag at least 5 h behind that of OVAp. CFSE dilution assays also revealed a similar lag in the proliferative response. These in vitro results fully comply with our in vivo observation using a different low affinity variant of the OVAp. Based on these findings a revised model of kinetic proofreading has been suggested in which activation by low affinity ligands results in full responsiveness by "trickling" through to less reversible downstream signaling intermediates (7). A possible candidate to act as a "counter" for productive TCR–ligand engagements is phosphorylated c-Jun, which was shown to slowly accumulate over time.

Whether reduced TCR signal strength may also account for the kinetic shift in response to the subdominant epitope of hCRP is unclear because the relative affinities of the TCR for their respective ligands has not be determined quantitatively. Alternatively, a lower density of the subdominant epitope resulting in a slower recruitment of a critical number of TCR may also delay the course of activation. Indeed, Iezzi et al. (5) showed that the timing of commitment to cell proliferation in vitro was dependent on the antigen dose. Surprisingly, we did not observe such a dose dependency in vivo. By lowering the antigen dose by a factor of 50 the relative onset and magnitude of the response to the dominant and subdominant response were unaltered. Additional fivefold reduction abolished the response. One reason for this critical dose threshold might be a nonlinear correlation between the dose of antigen applied peripherally and the dose arriving in the local LN. Moreover, by lowering the antigen dose, the number of antigen-laden APCs migrating to the node and the density of antigen per cell might be affected differentially. Thus, a critical number of antigen-laden APCs necessary to reach a response threshold may no longer be achieved below a certain threshold. A recent report estimated 3,000 APCs per LN to be sufficient to induce a CD8 response (18). Our results are reminiscent of a study on the effect of TCR density on the immune response. Lowering the density of the TCR on mature T cells by a factor of 20 had little effect on the antigen-specific response (40), an in vivo response threshold, which had not been predicted by previous in vitro studies (41).

The overall response toward the subdominant epitope (Fig. 5, compare left and right panels) and toward the weak agonist (Fig. 4, compare top and bottom right panels) was smaller when compared with the dominant epitopes. This might be a direct result of the delay in the initiation of proliferation. With antigen availability and the number of
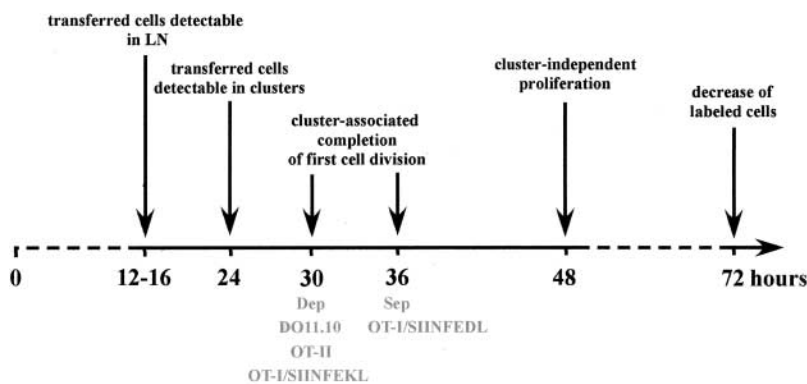
Figure 8. Summary of dynamic changes in T cell–APC clusters during the antigen-specific immune response in different experimental models.

transferred T cell precursors limited, a later start may recruit fewer T cells into the response.

Interestingly, cohorts of T cells having divided one to four times coexist in LNs 48 h after transfer. These different division rates might be explained in two ways. Either T cells initiate cell division at the same time but cease to divide after different rounds, or, alternatively, the onset of the first division varies (42). Thus, T cells entering the local LN after intravenous injection at different times will also engage in DC interactions sequentially. Only in the latter case can the proliferation of the earliest cohort be taken as a measure of the average cell cycle time of subsequent division rates. The calculated division time of 4.5 h accords well with previous estimates based on in vivo responses (19).

Notwithstanding subtle variations in the response kinetics of different TCR/ligand pairs, our data define a time frame for a sequential transit of T cells through a cell interaction–dependent compartment lasting ∼30–36 h followed by a second cell contact–independent phase lasting for another 24–36 h until T cells eventually exit the node (Figs. 6 and 8). Thus, the concept of sequential transit through such compartments, as recently deduced from in vitro studies (43), has been validated in vivo. Both phases encompass a time window originally defined by the sequestration of antigen-specific T cells from the circulation after immunization (44).

Lymphocyte–APC interactions not only serve the initial activation of CD4 T cells during the adaptive immune response, but also are the presumed site of mutual interactions between lymphocyte subsets via linked epitope recognition. These include CD4 T cell help for CD8 T and B cells, commitment of naive T cells to Th1 and Th2 (45, 46), and suppression of effector T cells by regulatory CD4 T cells (47). Depending on the specificity and lineage of the T cells and the differentiation stage of the DCs involved, these interactions may take part in an immune response or in the maintenance of self-tolerance (48). The tight packaging of cells in this confined microenvironment allows soluble factors in high concentrations to limit their target range to cells within such a cluster either via membrane contact or short-range diffusion (46). Here we show that such mixed clusters, which had been postulated on

theoretical grounds and reconstituted in vitro (13, 35), do exist in situ. Selected pairs of T cells specific for the same or a different antigen, when transferred into immunized mice, colocalized to the same cluster. Although less frequent than clusters harboring only one type of transferred cells, these mixed clusters most likely serve as ignition sites of the respective cell cooperation.

Cotransfer of different T cell populations interacting with the same APCs did not reveal mutual effects on the response of either population in this experimental setting. This may have several reasons. The relative high precursor frequency of antigen-specific T cells limits the extent of clonal proliferation and therefore may mask effects occurring at lower physiological precursor frequencies giving rise to larger clonal burst sizes (49). Second, based on their selection, the TCRs specific for the dominant and subdominant epitope of hCRP are likely to be of similar affinity and thus would compete equally well for limited binding sites on APCs (50). Mutual effects may only become apparent when certain parameters become limiting (e.g., space, soluble factors, or APC sites). We did indeed observe reciprocal effects on the response of both populations when antigen was limiting after delivery as a single pulse intravenously (unpublished data).

The approach introduced here complements the analysis of the intact microenvironment by recently developed imaging techniques. It allows multicellular clusters, which are formed in vivo as a result of highly specific, selective, and often rare interactions between mobile/resident cells to be analyzed in vitro with high resolution. These include distinct facets of the T and B cell response. In combination with fluorescent cell trackers and single cell staining for differentiation markers and effector molecules, this approach should yield new details of such confined microenvironments at the cellular and molecular level.

References

1. Banchereau, J., and R.M. Steinman. 1998. Dendritic cells and the control of immunity. *Nature*. 392:245–252.

2. Dustin, M.L., and A.C. Chan. 2000. Signaling takes shape in the immune system. *Cell*. 103:283–294.

3. Weiss, A. 1999. T-lymphocyte activation. *In* Fundamental Immunology, 4th edition. W.E. Paul, editor. Lippincott-Raven, Philadelphia/New York. 411–445.

4. van Stipdonk, M.J.B., E.E. Lemmens, and S.P. Schoenberger. 2001. Naive CTLs require a single brief period of antigenic stimulation for clonal expansion and differentiation. *Nat. Immunol.* 2:423–429.

5. Iezzi, G., K. Karjalainen, and A. Lanzavecchia. 1998. The duration of antigenic stimulation determines the fate of naive and effector T cells. *Immunity*. 8:89–95.

6. Gudmundsdottir, H., A.D. Wells, and L.A. Turka. 1999. Dynamics and requirements of T cell clonal expansion *in vivo* at the single cell level: effector function is linked to proliferative capacity. *J. Immunol.* 162:5212–5223.

7. Rosette, C., G. Werlen, M.A. Daniels, P.O. Holman, S.M. Alam, P.J. Travers, N.R. Gascoigne, E. Palmer, and S.C. Jameson. 2001. The impact of duration versus extent of TCR occupancy on T cell activation: a revision of the kinetic proofreading model. *Immunity*. 15:59–70.

8. Busch, D.H., I.M. Pilip, S. Vijh, and E.G. Pam. 1998. Coordinate regulation of complex T cell populations responding to bacterial infection. *Immunity*. 8:353–362.

9. Gunzer, M., A. Schafer, S. Borgmann, S. Grabbe, K.S. Zanker, E.B. Brocker, E. Kampgen, and P. Friedl. 2000. Antigen presentation in extracellular matrix: interactions of T cells with dendritic cells are dynamic, short-lived and sequential. *Immunity*. 13:323–332.

10. Inaba, K., S. Turley, F. Yamaide, T. Iyoda, K. Mahnke, M. Inaba, M. Pack, M. Subklewe, B. Sauter, D. Sheff, et al. 1998. Efficient presentation of phagocytosed cellular fragments on the major histocompatibility complex class II products of dendritic cells. *J. Exp. Med.* 188:2163–2173.

11. Ingulli, E., D.R. Ulman, M.M. Lucido, and M.K. Jenkins. 2002. *In situ* analysis reveals physical interactions between CD11b+ dendritic cells and antigen-specific CD4 T cells after subcutaneous injection of antigen. *J. Immunol.* 169:2247–2252.

12. Kyewski, B.A., R.V. Rouse, and H.S. Kaplan. 1982. Thymocyte rosettes: multicellular complexes of lymphocytes and bone marrow-derived stromal cells in the mouse thymus. *Proc. Natl. Acad. Sci. USA*. 79:5646–5650.

13. Inaba, K., M.D. Witmer, and R.M. Steinman. 1984. Clustering of dendritic cells, helper T lymphocytes, and histocompatible B cells during primary antibody responses in vitro. *J. Exp. Med.* 160:858–876.

14. Luther, S.A., A. Gulbranson-Judge, H. Acha-Orbea, and I. MacLennan. 1997. Viral superantigen drives extrafollicular and follicular B cell differentiation leading to virus-specific antibody production. *J. Exp. Med.* 185:551–562.

15. Kudo, S., K. Matsuno, T. Ezaki, and M. Ogawa. 1997. A novel migration pathway for rat dendritic cells from the blood: hepatic sinusoids-lymph translocation. *J. Exp. Med.* 185:777–784.

16. Saiki, T., E. Taichi, M. Ogawa, K. Maeda, H. Yagita, and K. Matsuno. 2001. *In vivo* roles of donor and host dendritic cells in allogeneic immune response: cluster formation with host proliferating cells. *J. Leukoc. Biol.* 69:705–712.

17. Ingulli, E., A. Mondino, A. Khoruts, and M.K. Jenkins. 1997. In vivo detection of dendritic cell antigen presentation to CD4+ cells. *J. Exp. Med.* 185:2133–2141.

18. Norbury, C.C., D. Malide, J.S. Gibbs, J.R. Bennik, and J.W. Yewdell. 2002. Visualizing priming of virus-specific CD8+ T cells by infected dendritic cells *in vivo*. *Nat. Immunol.* 3:265–271.

19. Stoll, S., J. Delon, T.M. Brotz, and R.N. Germain. 2002. Dynamic imaging of T cell-dendritic cell interactions in lymph nodes. *Science*. 296:1873–1876.

20. Miller, M.J., S.H. Wei, I. Parker, and M.D. Cahalan. 2002. Two-photon imaging of lymphocyte motility and antigen response in intact lymph node. *Science*. 296:1869–1873.

21. Kyewski, B.A. 1987. Seeding of thymic microenvironments defined by distinct thymocyte–stromal cell interactions is developmentally controlled. *J. Exp. Med.* 166:520–538.

22. Klein, L., T.C. Klein, U. Rüther, and B.A. Kyewski. 1998. CD4 T cell tolerance to human C-reactive protein, an inducible serum protein, is mediated by medullary thymic epithelium. *J. Exp. Med.* 188:5–16.

23. Barnden, M.J., J. Allison, W.R. Heath, and F.R. Carbone. 1998. Defective TCR expression in transgenic mice constructed using cDNA-based alpha- and beta-chain genes under the control of heterologous regulatory elements. *Immunol. Cell Biol.* 76:34–40.

24. Hogquist, K.A., S.C. Jameson, W.R. Heath, J.L. Howard, M.J. Bevan, and F.R. Carbone. 1994. T cell receptor antagonist peptides induce positive selection. *Cell*. 76:17–27.

25. Shimonkevitz, R., S. Colon, J.W. Kappler, P. Marrack, and H.M. Grey. 1984. Antigen recognition by H-2-restricted T cells. II. A tryptic ovalbumin peptide that substitutes for processed antigen. *J. Immunol.* 133:2067–2074.

26. Jameson, S.C., F.R. Carbone, and M.J. Bevan. 1993. Clonespecific T cell receptor antagonists of major histocompatibility complex class I–restricted cytotoxic T cells. *J. Exp. Med.* 177:1541–1550.

27. Garcia De Vinuesa, C., A. Gulbranson-Judge, M. Khan, P. O'Leary, M. Cascalho, M. Wabl, G.G. Klaus, M.J. Owen, and I.C. MacLennan. 1999. Dendritic cells associated with plasmablast survival. *Eur. J. Immunol.* 11:3712–3721.

28. Balazs, M., F. Martin, T. Zhou, and J. Kearney. 2002. Blood dendritic cells interact with splenic marginal zone B cells to initiate T–independent immune responses. *Immunity*. 17:341–352.

29. Taub, R.N., A.R. Krantz, and D.W. Dresser. 1970. The effect of localized injection of adjuvant material on the draining lymph node. *Immunology*. 18:171–186.

30. Ager, A. 1997. Regulation of lymphocyte migration into lymph nodes by high endothelial venules. *Biochem. Soc. Trans.* 25:421–428.

31. Hara, T., L.K. Jung, J.M. Bjorndahl, and S.M. Fu. 1986. Human T cell activation. III. Rapid induction of a phosphorylated 28 kD/32 kD disulfide-linked early activation antigen (EA 1) by 12-*O*-tetra-decanoyl phorbol-13-acetate, mitogens, and antigens. *J. Exp. Med.* 164:1988–2005.

32. Klein, T.C., T. Döffinger, M.B. Pepys, U. Rüther, and B.A. Kyewski. 1995. Tolerance and immunity to the inducible self-antigen C-reactive protein in transgenic mice. *Eur. J. Immunol.* 25:3489–3495.

33. Döffinger, R., T.C. Klein, M.B. Pepys, J.L. Casanova, and B.A. Kyewski. 1997. The MHC class II-restricted T cell response of C57BL/6 mice to human C-reactive protein: homology to self and the selection of T cell epitopes and T cell receptors. *Mol. Immunol.* 34:115–124.

34. Kaech, S.M., and R. Ahmed. 2001. Memory CD8+ T cell differentiation: initial antigen encounter triggers a developmental program in naive cells. *Nat. Immunol.* 2:416–422.

35. Mitchison, N.A. 1990. An exact comparison between the efficiency of two- and three-cell-type clusters in mediating helper activity. *Eur. J. Immunol.* 20:699–702.

36. Waldman, H., and S. Cobbold. 2001. Regulating the immune response to transplants: a role for CD4+ regulatory cells. *Immunity.* 14:399–406.

37. Zinkernagel, R.M., S. Ehl, P. Aichele, S. Oehen, T. Kundig, and H. Hengartner. 1997. Antigen localization regulates immune responses in a dose- and time-dependent fashion: a geographical view of immune reactivity. *Immunol. Rev.* 156: 199–209.

38. Chao, C.C., R. Jensen, and M.O. Dailey. 1997. Mechanisms of L-selectin regulation by activated T cells. *J. Immunol.* 159: 1686–1694.

39. Underhill, D.M., M. Bassetti, A. Rudensky, and A. Aderem. 1999. Dynamic interactions of macrophages with T cells during antigen presentation. *J. Exp. Med.* 190:1909–1914.

40. Labrecque, N., L.S. Whitfield, R. Obst, C. Waltzinger, C. Benoist, and D. Mathis. 2001. How much TCR does a T cell need? *Immunity.* 15:71–82.

41. Viola, A., and A. Lanzavecchia. 1996. T cell activation determined by T cell receptor number and tunable thresholds. *Science.* 273:104–106.

42. Gett, A.V., and P.D. Hodgkin. 2000. A cellular calculus for signal integration by T cells. *Nat. Immunol.* 1:239–244.

43. Jelley-Gibbs, D.M., N.M. Lepak, M. Yen, and S.L. Swain. 2000. Two distinct stages in the transition from naive CD4 T cells to effectors, early antigen-dependent and late cytokine-driven expansion and differentiation. *J. Immunol.* 165:5017–5026.

44. Sprent, J., J.F. Miller, and G.F. Mitchell. 1971. Antigen-induced selective recruitment of circulating lymphocytes. *Cell. Immunol.* 2:171–181.

45. Moser, M., and K.M. Murphy. 2000. Dendritic cell-regulation of Th1-Th2 development. *Nat. Immunol.* 1:199–205.

46. Kourilsky, P., and P. Truffa-Bachi. 2001. Cytokine fields and the polarization of the immune response. *Trends Immunol.* 22: 502–509.

47. Maloy, K.J., and F. Powrie. 2001. Regulatory T cells in the control of immune pathology. *Nat. Immunol.* 2:816–822.

48. Steinman, R.M., and M.C. Nussenzweig. 2002. Avoiding horror autotoxicus: the importance of dendritic cells in peripheral T cell tolerance. *Proc. Natl. Acad. Sci. USA.* 99:351–358.

49. Smith, A.L., M.E. Wikstrom, and B. Fazekas de StGroth. 2000. Visualizing T cell competition for peptide/MHC complexes: a specific mechanism to minimize the effect of precursor frequency. *Immunity.* 13:783–794.

50. Kedl, R.M., W.A. Rees, D.A. Hildeman, B. Schaefer, T. Mitchell, J. Kappler, and P. Marrack. 2000. T cells compete for access to antigen-bearing antigen-presenting cells. *J. Exp. Med.* 192:1105–1113.

The Journal of Experimental Medicine